

RESULTS OF A STUDY ON POLARIZATION MIX SELECTION FOR THE NSCAT SCATTEROMETER

David G. Long R. Scott Dunbar Scott Shaffer
Michael H. Freilich S. Vincent Hsiao

Jet Propulsion Laboratory, California Institute of Technology
4800 Oak Grove Dr., Pasadena, CA 91109

ABSTRACT

The NASA Scatterometer (NSCAT) is an instrument designed to measure the radar backscatter of the ocean's surface for estimating the near-surface wind velocity. A given resolution element is observed from several different azimuth angles. From these measurements the near-surface vector wind over the ocean may be inferred using a geophysical model function relating the normalized radar backscatter coefficient (σ^0) to the near-surface wind. The nature of the model function (i.e., upwind σ^0 is nearly the same as the downwind σ^0) results in several ambiguous wind vector estimates. An ambiguity removal algorithm is typically used to select a unique wind vector estimate. The radar polarization used to make the σ^0 measurements affects both the accuracy of the resulting wind measurements and the ambiguity removal skill. While horizontal polarization σ^0 typically has larger azimuthal modulation and increased upwind/downwind asymmetry, the overall σ^0 levels are substantially lower (resulting in decreased SNR) relative to vertical polarization.

The NSCAT baseline design provides for a total of six dual-polarization fan-beam antennas, which are arranged to provide three azimuthal looks of each resolution element over a 600 km wide swath on each side of the spacecraft ground track. Each antenna may be used for either vertical or horizontal polarization measurements. A single antenna on each side of the spacecraft may be used with both polarizations. A particular assignment of polarizations to each antenna is known as the polarization mix. Earlier studies to select a polarization mix for NSCAT were based on a "compass"-type simulation and did not consider ambiguity removal performance. In this paper we report on the results of a study to select a polarization mix for NSCAT using an end-to-end simulation of the NSCAT scatterometer and ground processing of the σ^0 measurements into unambiguous wind fields using a median-filter-based ambiguity removal algorithm. For various polarization mixes, the system simulation was used to compare the wind measurement accuracy and ambiguity removal skill over a set of realistic meso-scale wind fields. Considerations in the analysis and simulation are discussed and a recommended polarization mix given.

1. INTRODUCTION

The spaceborne NSCAT instrument uses 6 fan-beam antennas to provide multiple azimuth angle observations of the normalized radar backscatter (σ_0) of each resolution element, termed a "wind vector cell". The measurements of σ^0 made by the instrument are used to infer the near-surface wind vector

using a geophysical model function such as SASS-1. Unfortunately, the bi-harmonic dependence of σ^0 on the wind direction results in several ambiguous estimates of the wind direction and an ambiguity removal algorithm is required to obtain a unique wind vector estimate (see Shaffer *et al.*, 1989).

The NSCAT antenna illumination pattern is shown in Fig. 1 (Long *et al.*, 1988). While each antenna may be used with both vertical and horizontal polarization, only 4 out of the possible 6 polarization beams on each side of the spacecraft will be used. Two of the antennas on each side will be used with only a single polarization; one antenna will operate with both vertical and horizontal polarization. Using all the beams would reduce the observation time available for each measurement of σ^0 and require a more complex antenna switching matrix which would introduce additional RF path loss. Both considerations result in significantly reduced σ^0 measurement accuracy.

The polarization mix used to make the σ^0 measurements affects both the accuracy of the wind estimate as well as the ability to resolve the inherent ambiguity in the wind direction estimate. In order to optimize the wind measurement performance of NSCAT, we wish to select the polarization mix which gives the best overall wind measurement performance. Previous studies (Chi, 1987) to select a polarization mix were based on a "compass"-type simulation which does not consider the ability of an ambiguity removal algorithm to correctly select the wind direction. For a given wind speed, the simulation uses Monte Carlo techniques to evaluate the wind measurement performance for wind directions "around the compass" at a single sample point within the measurement swath. In the compass simulation, the ambiguity closest to the true wind is used to compute the measurement error. This technique gives the scatterometer measurement accuracy corresponding to perfect selection of the ambiguity closest to the true wind vector, i.e., for ideal ambiguity removal.

The compass simulation can be used to evaluate the instrument skill but not the ambiguity removal skill since ambiguity removal algorithms typically use nearby measurements of the wind vector and assumptions about the spatial correlation of the wind field. Instrument skill is the percentage of occurrences in which with the highest likelihood ambiguity corresponds to the ambiguity closest to the true wind vector. Algorithm skill is the percentage of correct selections (i.e., selection of the ambiguity closest to the true wind) made by the ambiguity removal algorithm.

Using the compass simulation with the instrument skill and the root-mean-square (RMS) wind speed and direction error as metrics, an initial selection of a baseline polarization mix for

NSCAT was made (Chi, 1987). The selected baseline antenna polarization mix utilized both polarizations for antennas 2 and 5 and vertical polarization for the remaining antennas (refer to Fig. 1). The resulting sequence of antenna beams used to make σ° measurements is: 1V 6V 2V 5V 2H 5H 3V 4V, where V indicates vertical polarization, H indicates horizontal polarization.

Since the ambiguity removal skill depends on the polarization mix, the final selection of the polarization mix must consider the ambiguity removal skill. We have developed an end-to-end system simulation of NSCAT which includes ambiguity removal. In this simulation, the scatterometer is "flown" over realistic wind fields. The changing orbital geometry is included. Monte Carlo techniques are used to generate measurement noise, geophysical modelling error, and σ° retrieval error. A point-wise maximum-likelihood wind retrieval technique is used (Chi and Li, 1988) to generate ambiguous winds. The ambiguous wind fields are processed by the NSCAT baseline median-filter-based ambiguity removal algorithm described in Shaffer *et al.*, 1989. This simulation has been used to evaluate all possible polarization mixes for NSCAT to select the polarization mix which provides the best overall performance.

2. SIMULATION PROCEDURE

As input to the system simulation, high resolution meso-scale surface wind fields are required. Since little conventional mesoscale wind field data over the ocean is available, simulated wind fields were generated. As described in Bevan and Freilich, 1987, original ECMWF surface wind fields at 1.875 deg resolution were interpolated to 10 km and non-divergent small-scale variability with a ak^{-2} spectrum (see Freilich and Chelton, 1987) was added. For a given 2000×2000 km region, the value of a was selected to be consistent with the spectrum within the region. Twelve wind fields were selected to span a wide range of meteorological conditions. The distribution of wind speeds and directions contained within the twelve wind files used for this study is depicted in Figure 2. The wind speed distribution is approximately Rayleigh for each wind direction.

Figure 3 illustrates the twelve polarization mixes considered (the left-side beam polarization mix is obtained by symmetry [see Fig. 1]). The algorithm to evaluate each polarization mix is described here. Using the system simulation, σ° measurements corresponding to each wind field and polarization mix were generated. These were then processed into ambiguous winds. The set of twelve wind fields were divided into two groups. For each polarization, the first group of six were used to select the optimum median-filter-based ambiguity removal algorithm parameters using the procedure described in Shaffer *et al.*, 1989. The resulting optimum ambiguity removal parameters for each polarization mix are shown in Table 1. An equally-weighted square window was used. For mode 0 only the wind direction was considered for ambiguity selection while for mode 1 a vector criterion was used. The likelihood weighting factor is indicated under "likelihood" (see Shaffer *et al.*, 1989).

The second, withheld group of 6 wind files were then processed using the ambiguity removal algorithm with the appropriate optimum parameters. For each polarization mix, the wind measurement performance was then determined over all twelve wind files. The performance metrics used were the algorithm skill, an ambiguity selection error "clumpiness" metric, and the RMS wind retrieval error for both speed and direction. The clumpiness metric is obtained by calculating the percentage of 12 by 12 wind cell regions which have better than 85% algorithm skill (see Shaffer *et al.*, 1989).

3. SIMULATION RESULTS

The results of the twelve polarization mixes are listed in Tables 2 through 4. The algorithm skill, clumpiness, and the RMS wind speed and direction errors, averaged over all 12 wind fields are shown in Table 2. The wind speed and direction errors are shown for both the closest ambiguity to the truth ("closest") and the ambiguity selected by the ambiguity removal algorithm ("dealias"). This latter error can be expected to be equal or greater than the closest ambiguity error due to ambiguity selection errors.

The baseline polarization mix (number 1) has the highest algorithm skill and is second in both clumpiness and RMS wind direction error. While polarization mix 6 achieves the best measure of clumpiness and RMS dealiased wind direction error, it also has the largest RMS closest wind error, making it a poor choice overall. Polarization mix 2 has the best RMS closest wind error, but mediocre performance in the other categories. Polarization mix 1 is considered "best" overall.

Tables 3-6 separate the results into four different wind speed regimes; 3-6, 6-10, 10-15, and 15-30 m/s. Most global winds can be expected to fall in the 3-6 and 6-10 m/s regimes. For these tables, the clumpiness metric is not shown since there are few 12×12 regions which fall into a single wind speed regime. From these tables, we note the dependence of the ambiguity removal skill on wind speed. The baseline polarization mix has a substantially higher algorithm skill than the other mixes at low wind speed. While polarization mix 6 has a better algorithm skill than the baseline mix 1 above 10 m/s, it has poor RMS closest direction error. Because there are fewer wind vectors which fall into the higher wind speed regimes, these categories do not contribute as much to the overall performance metrics summarized in Table 2. Based on the results presented in Tables 2-6, the baseline polarization mix (mix 1) is recommended as the overall best for use on NSCAT.

4. CONCLUSION

In this paper, we have reported on the results of a study to select a polarization mix for NSCAT. Based on the simulated results, polarization mix 1 (see Fig. 1) is recommended. The results are based on ambiguity removal and wind measurement accuracy performance considerations obtained using simulated wind fields with the SASS-1 geophysical model function. Similar performance is obtained with other model functions such as WENTZ (Wentz *et al.*, 1984). Further analysis will assess the impact of the choice of model function, failure of an antenna beam, and calibration considerations.

5. ACKNOWLEDGEMENTS

The research contained in this paper was performed at the Jet Propulsion Laboratory, California Institute of Technology, under contract with the National Aeronautics and Space Administration.

REFERENCES

1. Bevan, R., and M. Freilich, "Wind Fields for BIGSIM", JPL internal memo NSCAT/MHF 87-15, October 1, 1987.
2. Chi, C., "Tradeoff Study of Various Antenna Polarization Selections for the NROSS Scatterometer Using the SASS-1 Model — Progress Report 3", JPL internal memo 3343-84-043, April 11, 1984.
3. Chi, C., and F. Li, "A Comparative Study of Several Wind Estimation Algorithms for Spaceborne Scatterom-

eters," *IEEE Transactions on Geoscience and Remote Sensing*, Vol. 26, No. 2, March 1988.

4. Freilich, M. H. and D. B. Chelton, "Wavenumber Spectra of Pacific Winds Measured by the Seasat Scatterometer," *Journal of Physical Oceanography*, Vol. 16, No. 4, pp. 741-757, April 1986.
5. Shaffer, S., R. S. Dunbar, S. V. Hsiao, and D. G. Long, "Selection of Optimum Median-Filter-Based Ambiguity Removal Algorithm Parameter Values for NSCAT," to be presented at the International Geoscience and Remote Sensing Symposium, 1989.
6. F. J. Wentz, S. Peteherych, and L.A. Thomas, "A Model Function for Ocean Radar Cross-sections at 14.6 GHz," *Journal of Geophysical Research*, Vol. 89, pp. 3689-3704, 1984.

Figure 1

NSCAT illumination pattern. Recommended polarization mix is indicated.

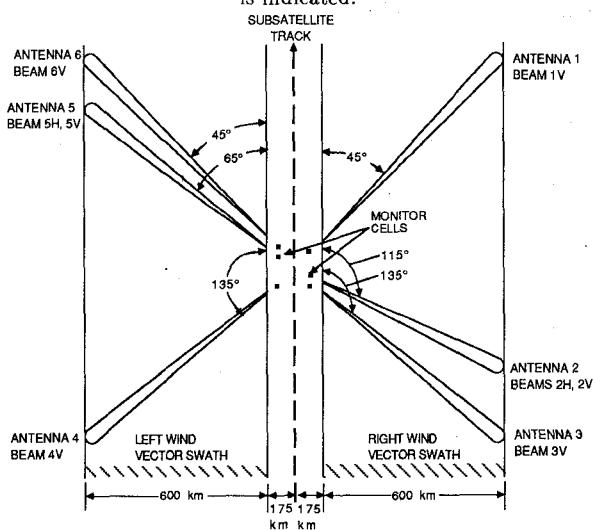


Figure 3

Beam polarization mixes considered.

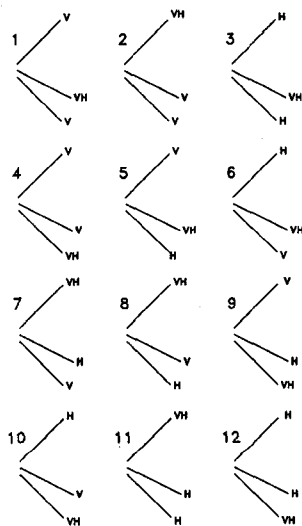


Figure 2

Histogram of the wind vectors in the twelve simulated mesoscale wind fields.

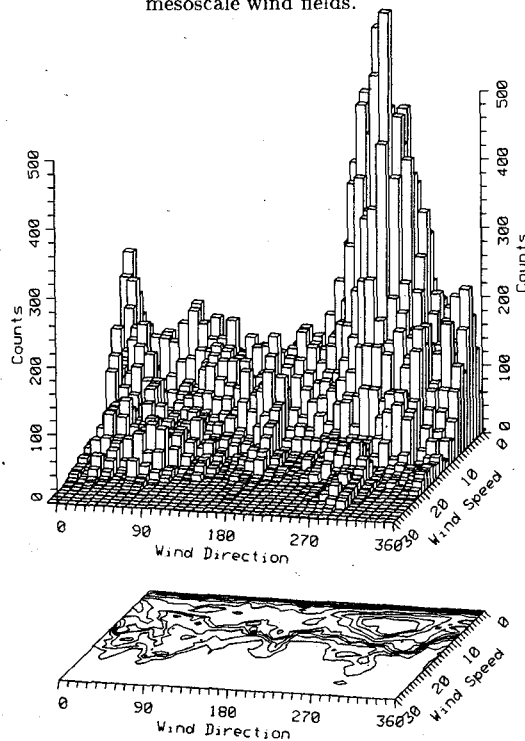


Table 1

Optimum Ambiguity Removal Parameters

Polarization Mix	Ambiguity Removal Size	Removal Mode	Parameters Likelihood
1	1V 2H 2V 3V	7x7	1 2.0
2	1V 1H 2V 3V	9x9	1 1.0
3	1H 2H 2V 3H	9x9	1 2.0
4	1V 2V 3V 3H	9x9	1 3.0
5	1V 2V 2H 3H	9x9	1 3.0
6	1H 2V 2H 3V	7x7	0 1.0
7	1V 1H 2H 3V	9x9	1 2.0
8	1V 1H 2V 3H	7x7	1 2.0
9	1V 2H 3V 3H	7x7	1 3.0
10	1H 2V 3V 3H	9x9	0 3.0
11	1V 1H 2H 3H	9x9	1 3.0
12	1H 2H 3V 3H	7x7	0 2.0

Table 2

Polarization Mix Performance

Polarization Mix	Algorithm Skill %	Clumpiness %	RMS Spd. Dealias	Err m/s Closest	RMS Dir. Dealias	Err ° Closest
1	96.0	98.14	0.69	0.68	28.24	10.46
2	91.5	91.34	0.66	0.62	43.23	9.88
3	88.9	94.96	0.75	0.70	42.43	14.38
4	94.3	97.18	0.67	0.66	34.14	10.43
5	88.6	92.61	0.71	0.67	46.02	10.84
6	95.0	99.42	0.73	0.71	28.20	14.42
7	89.3	90.94	0.66	0.62	46.93	10.32
8	91.4	94.99	0.70	0.63	38.66	10.48
9	91.1	95.54	0.67	0.65	44.42	10.77
10	93.5	97.85	0.73	0.70	35.50	14.63
11	79.6	80.13	0.77	0.62	65.94	11.92
12	89.4	94.94	0.73	0.67	46.21	14.95

Table 3
Polarization Mix Performance: 3 - 6 m/s

Polarization Mix	Algorithm Skill %	RMS Spd. Err m/s		RMS Dir. Err °	
		Dealias	Closest	Dealias	Closest
1 1V 2V 2H 3V	93.0	0.45	0.42	36.94	11.67
2 1V 1H 2V 3V	87.4	0.49	0.41	49.42	11.31
3 1H 2H 2V 3H	73.1	0.71	0.52	65.56	17.13
4 1V 2V 3V 3H	88.2	0.48	0.42	49.56	11.72
5 1V 2V 2H 3H	74.4	0.60	0.43	68.52	11.87
6 1H 2V 2H 3V	89.3	0.60	0.52	38.80	17.42
7 1V 1H 2H 3V	81.0	0.50	0.40	61.87	11.57
8 1V 1H 2V 3H	81.1	0.56	0.43	58.33	11.81
9 1V 2H 3V 3H	82.5	0.50	0.41	60.94	11.92
10 1H 2V 3V 3H	84.7	0.66	0.53	54.03	18.04
11 1V 1H 2H 3H	61.0	0.73	0.44	89.55	13.97
12 1H 2H 3V 3H	76.2	0.69	0.51	69.97	18.35

Table 4
Polarization Mix Performance: 6 - 10 m/s

Polarization Mix	Algorithm Skill %	RMS Spd. Err m/s		RMS Dir. Err °	
		Dealias	Closest	Dealias	Closest
1 1V 2V 2H 3V	98.1	0.59	0.59	17.56	9.65
2 1V 1H 2V 3V	93.6	0.57	0.53	37.65	9.05
3 1H 2H 2V 3H	95.0	0.61	0.59	29.72	13.36
4 1V 2V 3V 3H	96.5	0.57	0.57	26.66	9.62
5 1V 2V 2H 3H	94.8	0.58	0.57	30.36	10.00
6 1H 2V 2H 3V	96.8	0.63	0.62	24.78	13.54
7 1V 1H 2H 3V	91.0	0.56	0.52	43.42	9.48
8 1V 1H 2V 3H	95.8	0.56	0.54	26.32	9.73
9 1V 2H 3V 3H	94.6	0.56	0.55	34.19	9.89
10 1H 2V 3V 3H	97.0	0.62	0.61	24.19	13.52
11 1V 1H 2H 3H	84.4	0.68	0.52	59.73	10.90
12 1H 2H 3V 3H	94.4	0.61	0.58	32.65	13.63

Table 5
Polarization Mix Performance: 10 - 15 m/s

Polarization Mix	Algorithm Skill %	RMS Spd. Err m/s		RMS Dir. Err °	
		Dealias	Closest	Dealias	Closest
1 1V 2V 2H 3V	97.9	0.81	0.80	18.84	10.08
2 1V 1H 2V 3V	94.3	0.75	0.72	37.02	9.27
3 1V 2H 2V 3H	97.7	0.79	0.79	21.28	12.38
4 1V 2V 3V 3H	97.7	0.77	0.77	19.73	9.86
5 1V 2V 2H 3H	94.8	0.79	0.79	31.24	10.54
6 1V 2V 2H 3V	98.8	0.82	0.81	14.71	12.01
7 1V 1H 2H 3V	94.2	0.75	0.74	33.84	9.91
8 1V 1H 2V 3H	95.4	0.82	0.73	26.39	9.86
9 1V 2H 3V 3H	95.5	0.77	0.77	32.32	10.61
10 1H 2V 3V 3H	98.5	0.77	0.77	17.41	11.80
11 1V 1H 2H 3H	94.6	0.78	0.73	32.72	10.95
12 1H 2H 3V 3H	96.9	0.77	0.77	22.61	12.29

Table 6
Polarization Mix Performance: 15 - 30 m/s

Polarization Mix	Algorithm Skill %	RMS Spd. Err m/s		RMS Dir. Err °	
		Dealias	Closest	Dealias	Closest
1 1V 2V 2H 3V	94.9	1.18	1.19	37.03	10.45
2 1V 1H 2V 3V	94.8	1.07	1.06	38.55	10.12
3 1H 2H 2V 3H	98.7	1.18	1.19	16.36	12.71
4 1V 2V 3V 3H	98.0	1.17	1.18	21.41	10.72
5 1V 2V 2H 3H	97.8	1.17	1.17	24.21	11.47
6 1H 2V 2H 3V	99.6	1.20	1.21	12.16	11.92
7 1V 1H 2H 3V	97.5	1.09	1.10	23.85	10.47
8 1V 1H 2V 3H	94.8	1.20	1.09	29.71	10.40
9 1V 2H 3V 3H	95.6	1.15	1.16	33.83	11.26
10 1H 2V 3V 3H	99.3	1.18	1.18	13.48	12.61
11 1V 1H 2H 3H	96.2	1.12	1.10	28.77	11.17
12 1H 2H 3V 3H	98.2	1.14	1.14	17.10	12.81